IOP PUBLISHING NANOTECHNOLOGY
Nanotechnology **18** (2007) 505705 (7pp) doi:10.1088/0957-4484/18/50/505705

Quantitative characterization of the formation of an interpenetrating phase composite in polystyrene from the percolation of multiwalled carbon nanotubes

Arun K Kota[1], Bani H Cipriano[2], Dan Powell[3], Srinivasa R Raghavan[2] and Hugh A Bruck[1,4]

[1] Department of Mechanical Engineering, University of Maryland, College Park, MD 20742, USA
[2] Department of Chemical and Biomolecular Engineering, University of Maryland, College Park, MD 20742, USA
[3] NASA-Goddard Space Flight Center, Greenbelt, MD 20771, USA

E-mail: bruck@eng.umd.edu

Received 29 June 2007, in final form 19 October 2007
Published 20 November 2007
Online at stacks.iop.org/Nano/18/505705

Abstract

For the first time, an interpenetrating phase polymer nanocomposite formed by the percolation of multiwalled carbon nanotubes (MWCNTs) in polystyrene (PS) has been quantitatively characterized through electrical conductivity measurements and melt rheology. Both sets of measurements, in conjunction with scanning electron microscopy (SEM) images, indicate the presence of a continuous phase of percolated MWCNTs appearing at particle concentrations exceeding 2 vol% MWCNTs in PS. To quantify the amount of this continuous phase present in the PS/MWCNT composite, electrical conductivity data at various MWCNT concentrations, β, are correlated with a proposed *degree of percolation*, $\bar{C}(\beta)$, developed using a conventional power-law formula with and without a percolation threshold. To quantify the properties of the interpenetrating phase polymer nanocomposite, the PS/MWCNT composite is treated as a combination of two phases: a continuous phase consisting of a pseudo-solid-like network of percolated MWCNTs, and a continuous PS phase reinforced by non-interacting MWCNTs. The proposed degree of percolation is used to quantify the distribution of MWCNTs among the phases, and is then used in a rule-of-mixtures formulation for the storage modulus, $G'(\beta, \bar{C}(\beta), \omega)$, and the loss modulus, $G''(\beta, \bar{C}(\beta), \omega)$, to quantify the properties of the continuous phase consisting of percolated MWCNTs and the continuous PS phase reinforced by non-interacting MWCNTs from the experimental melt rheology data. The properties of the continuous phase of percolated MWCNTs are indicative of a scaffold-like microstructure exhibiting an elastic behavior with a complex modulus of 360 kPa at lower frequencies and viscoplastic behavior with a complex viscosity of 6 kPa s rad^{-1} at higher frequencies, most likely due to a stick–slip friction mechanism at the interface of the percolated MWCNTs. Additional evidence of this microstructure was obtained via scanning electron microscopy. This research has important implications in providing a new methodology based on the electrical and rheological properties of the polymer nanocomposite for quantifying the continuous phase formed by the percolation of new functionalized nanostructures being developed for: (a) controlling the percolation of the nanostructures through self-assembly, (b) enhancing their interaction with the continuous reinforced polymer phase, (c) enhancing the cohesion between nanostructures.

[4] Author to whom any correspondence should be addressed.

1. Introduction

Polymer composites based on carbon nanotubes (CNTs) are attracting attention due to their remarkable mechanical, thermal and electrical properties. The high aspect ratio of CNTs allows property enhancement at lower concentrations [1] as compared to conventional particles such as carbon black or nanoclays. Our motivation for this work is the potential use of polymer/CNT composites as conductive, strong, and yet lightweight materials in the civilian space arena. In our study, we employ multiwalled carbon nanotubes (MWCNTs), which are 50–200 nm in diameter, and are available at desirable quantities at an affordable cost. We add these particles to polystyrene (PS), a commodity plastic that is useful for applications such as radiation shielding, due to its relatively high content of hydrogen. The resulting PS/MWCNT composites are processed from solution and characterized for their rheological properties, electrical conductivity, and microstructure. Together, these techniques provide insight into the nanoscale structure and organization of the MWCNTs in the PS matrix.

PS/CNT composites have been studied recently by a few authors. Qian *et al* [1, 2] fabricated PS/MWCNT films by solvent evaporation and reported a 42% increase in the elastic modulus due to the particles. Thostenson *et al* [3] utilized solvent evaporation followed by microscale twin screw extrusion to obtain highly aligned PS/MWCNT films that exhibited a 49% increase in elastic modulus. Andrews *et al* [4] produced PS/MWCNT composites via melt mixing and reported a good dispersion with an electrical percolation at 0.25 vol%. Safadi *et al* [5] prepared PS/MWCNT films via spin casting and reported a transformation from insulating to conducting and a 100% increase in the tensile modulus at 5 wt%. Finally, Mitchell *et al* [6] added functionalized single-wall carbon nanotubes (SWCNTs) to PS and studied the melt rheology of the composites. They demonstrated the presence of a percolated network of SWCNTs at concentration exceeding 1.5 wt%.

Previously, we conducted a thorough melt rheology study of PS/MWCNT composites and compared the effects of solvent processing on the electrical and rheological percolation [7]. Similar systematic rheological studies have also been conducted, however, for MWCNT composites based on polycarbonate (PC) [8, 9], polyethylene (PE) [10], and polymethylmethacrylate (PMMA) [11]. In earlier works, the increase in electrical conductivity [11–16] and rheological parameters [11–13, 17] of polymer/CNT composites were each reported or modeled independently as a function of the particle percolation. However, to the best of our knowledge, there were no reports of a physical and quantitative relationship between the increase in electrical conductivity and rheological parameters, both of which fundamentally depend on the extent of particle percolation.

In this paper, for the first time, an interpenetrating phase polymer nanocomposite formed by the percolation of MWCNTs in PS/MWCNT composites is quantitatively characterized. This is accomplished by treating the PS/MWCNT composite as a combination of two phases: a continuous PS phase reinforced by non-interacting MWCNTs, and a continuous phase consisting of the pseudo-solid-like network of percolated MWCNTs. The distribution of MWCNTS among the continuous phases is determined from the degree of percolation of MWCNTs correlated with power-law fits of the electrical conductivity with and without a percolation threshold. Subsequently, the dynamic rheological properties (the storage modulus and loss modulus) of the PS/MWCNT composites are interpreted as a function of the degree of percolation, in addition to the concentration of MWCNTs and frequency. This allows determination of the properties of the reinforced PS phase and the percolated MWCNT phase independently.

2. Experimental methods

A commercial polydisperse PS (molecular weight ∼150 000, polydispersity ∼2.73, density ∼1.04 g cm^{-3}) was used in this work from Nova Chemicals, and vapor grown, graphitized MWCNTs (diameter ∼50–200 nm, length ∼5–10 μm, density ∼0.6 g cm^{-3}) were used from the University of Kentucky, Lexington, KY (see figure 4(a)). The solvent, tetrahydrofuran (THF), was obtained from Fisher Scientific. PS/MWCNT composites were prepared by a solvent evaporation method. A dispersion of 5 wt% MWCNTs in THF was sonicated in an ultrasonic bath (VWR 75D) with occasional stirring. The dispersion of MWCNTs was added to a PS solution in the same solvent. The mixture was stirred and sonicated in a closed beaker alternately every 30 min for at least 6 h. As noted in an earlier work [12], it was observed that periodic addition of solvent produced better dispersion. The composite was obtained by solvent evaporation and dried for 12–24 h in a vacuum oven at 50 °C to remove the residual solvent. The dried composite was hot pressed into a disc of 2.5 cm diameter and 5 mm thickness at a temperature of 170 °C. Samples with 0, 0.01, 0.03, 0.05 and 0.07 mass fractions of MWCNTs in PS were prepared by this method.

The electrical conductivity of the composites was measured by a two-point probe technique in accordance with ASTM D4496. Samples of a known cross-sectional area and thickness were placed between copper electrodes and the DC resistance was measured using an Agilent 34401A precision digital multimeter. The measurements were made after the multimeter displayed a steady value, typically in 15 s. The surfaces of the sample in contact with the electrodes were coated with silver paint in order to reduce discrepancies arising from microroughness. It was ensured that the surface area of the electrodes exceeded the cross-sectional area of the discs.

Dynamic rheological measurements were performed on a Rheometrics RDAIII rheometer using 2.5 cm parallel plates. The melt rheology was done under a nitrogen atmosphere at a temperature of 190 °C with a gap of about 1 mm between the plates. The storage modulus and loss modulus were measured as functions of frequency (0.1–100 rad s^{-1}) within the linear viscoelastic regime of the sample. Each curve reported is an average of three different samples at a given concentration.

The microstructure of the surface of the samples was examined using a Quanta FEG 200 SEM. Previous studies [18, 19] have reported a charge accumulation on the composite surface, resulting in blurry images. This problem was circumvented without a metal coating on the surface by using a low energy electron beam (∼5 kV).

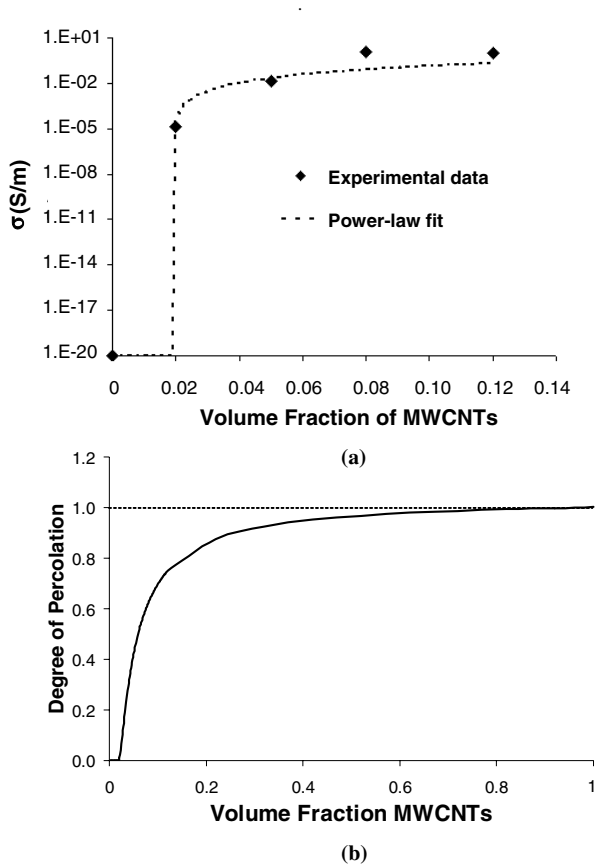

Figure 1. (a) Electrical conductivity of the nanocomposites at various MWCNT concentrations using fits from a classical power-law formula. (b) Degree of percolation at various MWCNT concentrations.

3. Results and discussion

3.1. Electrical conductivity measurements

Measurements of the conductivity of PS-MWCNT composites as a function of the MWCNT concentration can be seen in figure 1(a). Each data point on the plot represents the average of measurements on 6–8 different samples, and the scatter in the data was within 5% of this average value. The conductivity of pure PS is $\sim 10^{-20}$ S m^{-1}. Upon adding the MWCNTs, the conductivity of the composite increased by 20 orders of magnitude, approaching a value of 1 S m^{-1}. Such conductivity data are classically interpreted using the following power-law expression for the conductivity as a function of the particle volume fraction β:

$$\sigma_c^{\mathrm{PL}}(\beta) = \sigma_{\mathrm{PS}} + K(\beta - \beta_c)^{\lambda}. \tag{1}$$

Here, σ_c^{PL} is the conductivity of the composite determined by the power-law fit, σ_{PS} is the electrical conductivity of the pure PS, K is a constant based on the interconnectivity of the MWCNTs, β_c is the percolation threshold and λ is the critical exponent. The percolation threshold corresponds to the formation of a CNT network that allows electron transport by tunneling or electron hopping along CNT interconnects. The conductivity data for PS-MWCNT composites in figure 1(a) were fit to equation (1) using linear least squares analysis. The best-fit parameters are shown in table 1. For the fits, mass fractions (w) had to be converted to volume fractions (values in table 2) using a linear rule-of-mixtures as follows:

$$\beta = \frac{w\rho_{\mathrm{PS}}}{\rho_{\mathrm{MWNCT}} + w(\rho_{\mathrm{PS}} - \rho_{\mathrm{MWCNT}})}. \tag{2}$$

Here, ρ_{PS} is the density of PS and ρ_{MWCNT} is the density of MWCNTs.

Table 1. The best-fit power-law parameters for the electrical conductivity of PS/MWCNT composites.

Power-law parameter	THF (σ_c)
K	16
β_c	0.019
λ	1.9

Table 2. The relationship between mass and volume fractions for PS/MWCNT composites obtained using a linear rule-of-mixtures. Also shown is the degree of percolation calculated from the electrical conductivity measurement for each composition using the power-law fit.

Mass fraction	Volume fraction	Degree of percolation
0.01	0.02	0.00
0.03	0.05	0.42
0.05	0.08	0.62
0.07	0.12	0.75

3.2. Characterization of melt rheology

The melt rheology of the PS/MWCNT composites was investigated through dynamic rheological measurements. The storage modulus G' and the loss modulus G'' as functions of frequency can be seen in figure 2. It is clear that both G' and G'' increase with MWCNT concentration. At concentrations exceeding 2 vol%, G' reaches a plateau at low frequencies indicating that the percolated MWCNTs form a pseudo-solid-like network with strong interactions between polymer and particles [20, 21].

Similar to the electrical percolation threshold, rheological percolation is correlated with the onset of power-law dependence of a rheological property on the volume fraction. However, there is no agreement on which quantity to use in this regard: for example, while Du *et al* [11] report the percolation based on G', Kharchenko *et al* [17] report the percolation based on G'/G''. Furthermore, the onset of rheological percolation precedes electrical percolation according to some studies [11], while others have claimed that it occurs at a higher concentration [17].

In order to gain further insight into the relationship between electrical and rheological percolation, the PS/MWCNT composite is considered as a combination of two phases: a continuous PS phase reinforced by non-interacting MWCNTs, and a continuous phase consisting of a pseudo-solid-like network of percolated MWCNTs. In order to quantify the distribution

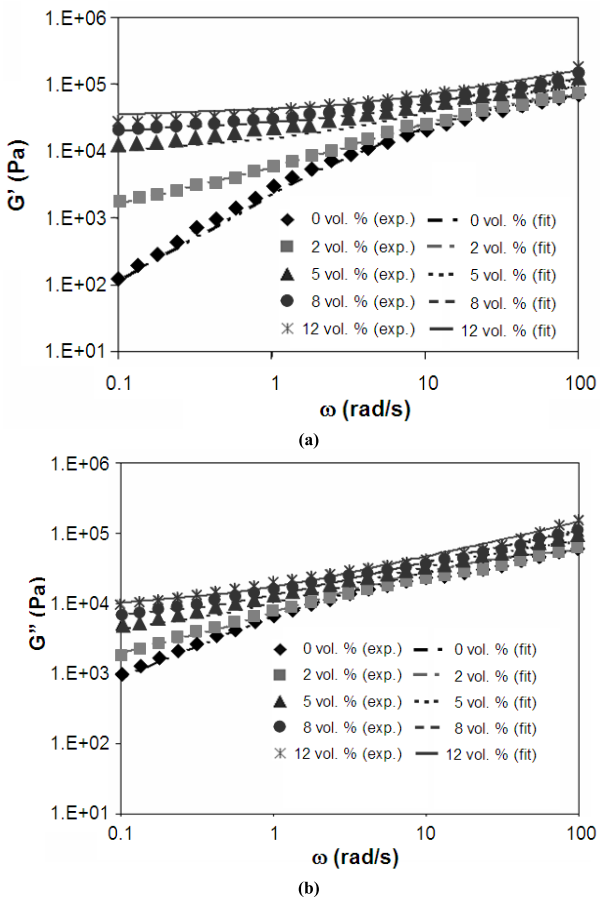

Figure 2. (a) Storage modulus (G') and (b) loss modulus (G'') of the composites as a function of frequency where the experimental data are symbols and the fits from the rheological model are lines. Data are shown for a range of MWCNT concentrations. Note that the fits from the proposed rheological model match well with the experimental data.

of MWCNTs among the phases, we propose the *degree of percolation* ($\bar{C}(\beta)$), defined as:

$$\bar{C}(\beta) = \frac{\sigma_c^{\mathrm{PL}}(\beta)}{\sigma_c^{\mathrm{PLPT0}}(\beta)}, \tag{3}$$

where $\sigma_c^{\mathrm{PLPT0}}(\beta)$ is the value of electrical conductivity according to the power-law fit when the percolation threshold is 0 vol% (i.e., instantaneous percolation). Thus, the degree of percolation reflects the offset in the connectivity of the MWCNTs that begins above the percolation threshold. The degree of percolation $\bar{C}(\beta)$ as a function of volume fraction can be seen in figure 1(b). The $\bar{C}(\beta)$ based on the power-law model converges to the theoretical maximum above a volume fraction of 0.6, which is close to the classical theoretical maximum packing fraction for cylinders of 0.79 where full percolation of the microstructure would have to occur. This indicates that the degree of percolation obtained from the power-law fit can provide a physically reasonable prediction of the distribution of MWCNTs among the interpenetrating phases. The degree of percolation corresponding to each of the compositions that was characterized is shown in table 2.

By using a linear rule-of-mixtures formulation commonly employed for predicting the properties of interpenetrating phase composites [22, 23], we propose to use a product of the degree of percolation and the volume fraction to quantify the contribution of each phase to the dynamic rheological properties of the composite: $\beta\bar{C}(\beta)$ for the continuous phase consisting of a pseudo-solid-like network of percolated MWCNTs and $1-\beta\bar{C}(\beta)$ for the continuous phase of PS reinforced by non-interacting MWCNTs. Accordingly, the storage modulus, G', and the loss modulus, G'', can each be represented as a function of the degree of percolation, $\bar{C}(\beta)$, frequency, ω, and MWCNT volume fraction, β, as shown in equations (4)–(9). The relationships in equations (4)–(9) are obtained from classical formulas used for describing the rheological response of polymers, including the effect of non-interacting particles and the viscoelastic behavior of a solid [24–29]. The continuous phase of percolated MWCNTs is modeled using a frequency dependent behavior of a elastic–viscoplastic solid observed in clay suspensions [25], while the unpercolated MWCNTs are modeled by using the classical Nielsen formula that introduces the concept of maximum packing using a generalized Kerner equation [29].

$$\begin{aligned} G'(\beta,\bar{C}(\beta),\omega) = {} & \beta\bar{C}(\beta)\Bigg[G'_{\mathrm{PMWCNT}}(0) \\ & + \eta'_{\mathrm{PMWCNT}}(\infty)\omega^c_{\mathrm{PMWCNT}}\Bigg(\Bigg(\frac{\omega}{\omega^c_{\mathrm{PMWCNT}}}\Bigg)^{.5} \\ & + \Bigg(\frac{\omega}{\omega^c_{\mathrm{PMWCNT}}}\Bigg)\Bigg)\Bigg] + (1-\beta\bar{C}(\beta)) \\ & \times\left[\frac{1+A\left(\frac{G'_{\mathrm{RMWCNT}}/G'_{\mathrm{PS}}(\omega)-1}{G'_{\mathrm{RMWCNT}}/G'_{\mathrm{PS}}(\omega)+A}\right)\varphi(\beta)}{1-\left(\frac{G'_{\mathrm{RMWCNT}}/G'_{\mathrm{PS}}(\omega)-1}{G'_{\mathrm{RMWCNT}}/G'_{\mathrm{PS}}(\omega)+A}\right)\varphi(\beta)\psi(\varphi(\beta))}\right]G'_{\mathrm{PS}}(\omega) \end{aligned} \tag{4}$$

$$\begin{aligned} G''(\beta,\bar{C}(\beta),\omega) = {} & \beta\bar{C}(\beta)\Bigg[G''_{\mathrm{PMWCNT}}(0) \\ & + \eta''_{\mathrm{PMWCNT}}(\infty)\omega^c_{\mathrm{PMWCNT}}\Bigg(\Bigg(\frac{\omega}{\omega^c_{\mathrm{PMWCNT}}}\Bigg)^{.5} \\ & + \Bigg(\frac{\omega}{\omega^c_{\mathrm{PMWCNT}}}\Bigg)\Bigg)\Bigg] + (1-\beta\bar{C}(\beta)) \\ & \times\left[\frac{1+A\left(\frac{G''_{\mathrm{RMWCNT}}/G''_{\mathrm{PS}}(\omega)-1}{G''_{\mathrm{RMWCNT}}/G''_{\mathrm{PS}}(\omega)+A}\right)\varphi(\beta)}{1-\left(\frac{G''_{\mathrm{RMWCNT}}/G''_{\mathrm{PS}}(\omega)-1}{G''_{\mathrm{RMWCNT}}/G''_{\mathrm{PS}}(\omega)+A}\right)\varphi(\beta)\psi(\varphi(\beta))}\right]G''_{\mathrm{PS}}(\omega), \end{aligned} \tag{5}$$

where,

$$G'_{\mathrm{PS}}(\omega) = G^p_{\mathrm{PS}}\frac{\left(\frac{\omega}{\omega^c_{\mathrm{PS}}}\right)^{2p}}{\left(1+\left(\frac{\omega}{\omega^c_{\mathrm{PS}}}\right)^p\right)^2} \tag{6}$$

$$G''_{\mathrm{PS}}(\omega) = \eta_{\mathrm{PS}}(0)\frac{\omega}{\left(1+\left(\frac{\omega}{\omega^c_{\mathrm{PS}}}\right)^q\right)^2} \tag{7}$$

$$\psi(\varphi(\beta)) = 1+(1-\varphi_m)\varphi(\beta)/\varphi_m^2 \tag{8}$$

$$\varphi(\beta) = (\beta-\beta\bar{C})/(1-\beta\bar{C}) \tag{9}$$

and the following constants are determined by applying equations (4)–(7) to the experimental melt rheology data:

$G'_{\text{PMWCNT}}(0)$	storage modulus of the continuous phase of percolated MWCNTs as $\varpi \to 0$
$\eta'_{\text{PMWCNT}}(\infty)$	real part of complex viscosity for the continuous phase of percolated MWCNTs as $\varpi \to \infty$
G'_{RMWCNT}	effective storage modulus of the MWCNT reinforcement in the continuous PS phase
G^p_{PS}	plateau modulus of pure PS
$G''_{\text{PMWCNT}}(0)$	loss modulus of the continuous phase of percolated MWCNTs as $\varpi \to 0$
$\eta''_{\text{PMWCNT}}(\infty)$	imaginary part of complex viscosity for continuous phase of percolated MWCNTs as $\varpi \to \infty$
G''_{RMWCNT}	effective loss modulus of the MWCNT reinforcement in the continuous PS phase
$\eta_{\text{PS}}(0)$	viscosity of pure PS as $\varpi \to 0$
$p, q,$	power-law indices
$\omega^c_{\text{PS}}, \omega^c_{\text{PMWCNT}}$	critical frequencies related to the relaxation of pure PS and percolated MWCNTs
A	shape and orientation factor of reinforcement
φ_m	maximum theoretical volume fraction of non-interacting MWCNTs.

Thus, the degree of percolation obtained from the electrical conductivity measurements provides a means of distinguishing the effect of percolated and unpercolated MWCNTs. This essentially results in a modification of the Nielsen equation for unpercolated suspensions to include the effects of percolation.

The fits to the experimental data obtained from using the new rheological models and the degree of percolation can also be seen in figure 2. These results indicate a good correlation between the fits and the experimental data, and verify the appropriateness of the new rheological models for capturing the formation of the interpenetrating phase composite from the percolation of the MWCNTs. Thus, the new rheological models permit, for the first time, determination of the properties of the continuous phase consisting of a pseudo-solid-like network of percolated MWCNTs. These values can be seen in table 3. The continuous phase of percolated MWCNTs exhibits an elastic solid-like behavior at low frequencies with a complex modulus, $G^*_{\text{PMWCNT}}(0) = \sqrt{(G'_{\text{PMWCNT}}(0))^2 + (G''_{\text{PMWCNT}}(0))^2} = 360$ kPa, and then transitions at higher frequencies to a viscoplastic solid-like behavior with a complex viscosity, $\eta^*_{\text{PMWCNT}}(\infty) = \sqrt{(\eta'_{\text{PMWCNT}}(\infty))^2 + (\eta''_{\text{PMWCNT}}(\infty))^2} = 6$ kPa s rad^{-1}. Simultaneously, it is possible to isolate the effects of the non-interacting MWCNTs that reinforce the PS. The reinforcing MWCNTs behave like an elastic solid with an effective complex modulus, $G^*_{\text{RMWCNT}}(0) = \sqrt{(G'_{\text{RMWCNT}}(0))^2 + (G''_{\text{RMWCNT}}(0))^2} = 208$ kPa.

The frequency response at low and high frequencies provides direct insight into the nature of the continuous phase of percolated MWCNTs. The normalized complex modulus, $G^*(\omega)/G^*(0)$, and the normalized complex viscosity, $\eta^*(\omega)/\eta^*(0)$, seen in figure 3 are consistent with the frequency independent modulus of an elastic solid at low frequencies and frequency independent viscosity of a viscoplastic solid at high frequencies. This behavior is indicative of a scaffold-like microstructure that exhibits a stick–slip friction mechanism at higher frequencies similar to that observed above T_g in nanoparticle-reinforced polymer composites [30].

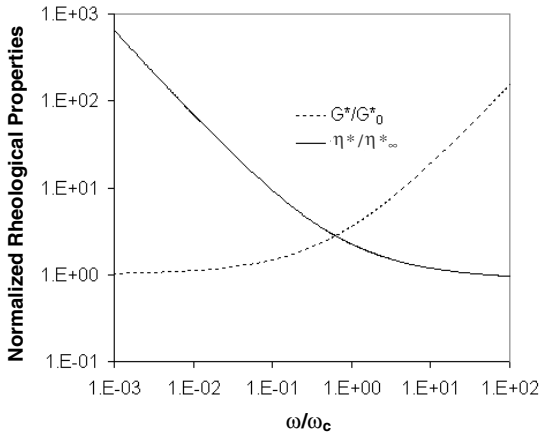

Figure 3. Normalized rheological properties of the continuous phase of percolated MWCNTs indicating elastic–viscoplastic behavior with a crossover in behavior from elastic to viscoplastic at the normalized frequency of 1.

Table 3. The values of the material properties determined from fitting experimental data for the PS/MWCNT composite with the new rheological models.

Constant	Value
$\eta'_{\text{PMWCNT}}(\infty)$	4 kPa s rad^{-1}
$G'_{\text{PMWCNT}}(0)$	350 kPa
G'_{RMWCNT}	200 kPa
G^p_{PS}	100 kPa
$\eta''_{\text{PMWCNT}}(\infty)$	5 kPa s rad^{-1}
$G''_{\text{PMWCNT}}(0)$	80 kPa
G''_{RMWCNT}	60 kPa
$\eta_{\text{PS}}(0)$	10 kPa s rad^{-1}
P	0.70
Q	0.55
ω^c_{PS}	12 rad s^{-1}
ω^c_{PMWCNT}	80 rad s^{-1}
A	1000
φ_m	0.65

This aspect of the research has an important implication in providing a new methodology for quantifying the continuous phase formed by the percolation of nanostructures in polymer nanocomposites through the properties obtained using equations (4)–(9). It can be applied to functionalized nanostructures being developed for [31, 32]: (a) controlling the percolation of the nanostructures through self-assembly, (b) enhancing their interaction with the continuous reinforced polymer phase, (c) enhancing the cohesion between nanostructures. This is possible because the continuous reinforced polymer phase stabilizes the state of the continuous phase of percolated nanostructures, which is similar in principle to the stabilization of proteins using formalin-fixed, paraffin-embedded tissue blocks for histopathology.

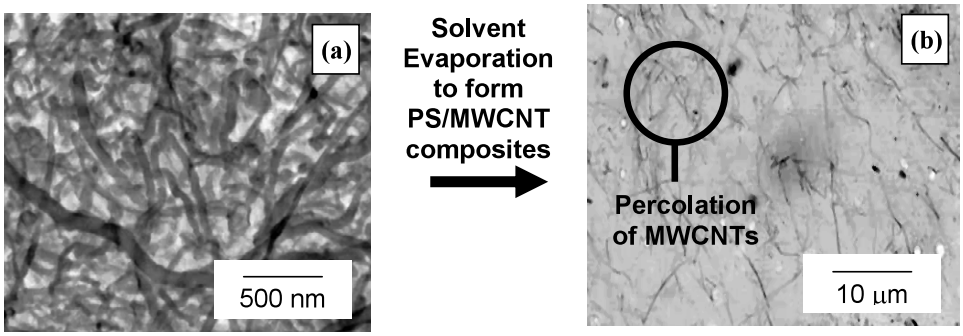

Figure 4. Scanning electron micrographs of: (a) an agglomeration of the as-received MWCNTs, and (b) the surface of an 8 vol% PS/MWCNT composite prepared by the solvent evaporation method indicating random dispersion and percolation of MWCNTs as also indicated by electrical conductivity measurements.

3.3. Microstructural characterization using scanning electron microscopy

The microstructure formed by the continuous phase of percolated MWCNTs was further studied using a scanning electron microscope (SEM). An agglomeration of the MWCNTs used in this work before they have been sonicated can be seen in figure 4(a). It was observed that the diameter ranged from 50 to 200 nm and the length ranged from 5 to 10 μm. The surface of the composite discs after hot-pressing revealed a random, isotropic dispersion of MWCNTs, as shown in figure 4(b) for the 8 vol% composite. The concentration of MWCNTs qualitatively appears to be consistent with volume fraction calculations, and the interconnectivity of the continuous phase of percolated MWCNTs resulting in the electrical and rheological percolation is also evident.

The microstructure characterized using SEM appears to possess scaffold-like characteristics. With a high aspect ratio (approximately 50:1), the MWCNTs appear to randomly overlap after the solvent evaporation process. With such a high aspect ratio, adhesion between the interconnected MWCNTs results in a frequency dependent cohesion at lower frequencies occurring over small contact areas across the percolated MWCNTs. At higher frequencies it is possible for small disturbances to cause separation due to a dynamic stick–slip friction mechanism. The micrographs obtained from the SEM also provide qualitative visual evidence of the scaffold-like microstructure of the continuous phase of percolated MWCNTs.

4. Conclusions

In summary, an interpenetrating phase polymer nanocomposite formed by the percolation of MWCNTs in PS was quantitatively characterized. The electrical conductivity measurements indicate that as the structure begins to percolate, the conductivity increases 20 orders of magnitude to 1 S m^{-1} at 12 vol% MWCNTs. To analyze the percolation behavior, the experimental data was fit using a classical power-law formula. Significant enhancements were also observed in the rheological properties of the PS/MWCNT composites due to the formation of the interpenetrating phases. At the low frequency limit, the storage modulus exhibited a predominant plateau at concentrations exceeding 2 vol%, indicating a pseudo-solid-like behavior due to percolation of the MWCNTs.

In order to elucidate on the relationship between the electrical and rheological percolation, the PS/MWCNT composite was treated as a combination of two phases: a continuous phase consisting of a pseudo-solid-like network of percolated MWCNTs, and a continuous PS phase reinforced by non-interacting MWCNTs. In order to quantify the distribution of MWCNTs among the phases, the *degree of percolation* was proposed from the power-law fit to the electrical conductivity data. The degree of percolation was used with a rule-of-mixtures formulation to determine the contribution of each continuous phase to the dynamic rheological properties of the PS/MWCNT composite.

For the first time, using the above proposed method, it was possible to determine the properties of the continuous phase of percolated MWCNTs. The continuous phase of percolated MWCNTs exhibits an elastic solid-like behavior at low frequencies with a complex modulus of 360 kPa, and then transitions at high frequencies to a viscoplastic solid-like behavior with a complex viscosity of 500 kPa s rad^{-1}. Simultaneously, it is possible to isolate the effect of non-interacting MWCNTs reinforcing the PS. The reinforcing MWCNTs behave like an elastic solid with a modulus of 208 kPa.

The frequency response at low and high frequencies provides direct insight into the nature of the continuous phase of percolated MWCNTs. The normalized complex modulus, $G^*(\omega)/G^*(0)$, and the normalized complex viscosity, $\eta^*(\omega)/\eta^*(0)$, are consistent with the frequency independent modulus of an elastic solid at low frequencies and frequency independent viscosity of a viscoplastic solid at high frequencies. This behavior is indicative of a scaffold-like microstructure that exhibits a stick–slip friction mechanism at the interface of the percolated MWCNTs at higher frequencies. Additional evidence of this microstructure was obtained via SEM.

Acknowledgment

The research in this paper was supported by NASA-Goddard Space Flight Center, Greenbelt, MD.

References

[1] Qian D and Dickey E C 2001 *J. Microsc.* **204** 39
[2] Qian D and Dickey E C 2002 *Appl. Phys. Lett.* **76** 2868
[3] Thostenson E T and Chou T-W 2002 *J. Phys. D: Appl. Phys.* **35** L77
[4] Andrews R, Jacques D, Minot M and Rantell T 2002 *Macromol. Mater. Eng.* **287** 395
[5] Safadi B, Andrews R and Grulke E A 2001 *J. Appl. Polym. Sci.* **84** 2660
[6] Mitchell C A, Bahr J L, Arepalli S, Tour J M and Krishnamoorti R 2002 *Macromolecules* **35** 8825
[7] Kota A, Cipriano B H, Duesterberg M, Gershon A L, Powell D, Raghavan S R and Bruck H A 2007 *Macromolecules* **40** 7400
[8] Potschke P, Brunig H, Janke A, Fischer D and Jehnichen D 2005 *Polymer* **46** 10355
[9] Potschke P, Fornes T D and Paul D R 2002 *Polymer* **43** 3247
[10] McNally T, Potschke P, Halley P, Murphy M, Martin D, Bell S E J, Brennan G P, Bein D, Lemoine P and Quinn J P 2005 *Polymer* **46** 8222
[11] Du F, Scogna R C, Zhou W, Brand S, Fischer J E and Winey K I 2004 *Macromolecules* **37** 9048
[12] Bryning M B, Islam M F, Kikkawa J M and Yodh A G 2005 *Adv. Mater.* **17** 1186
[13] Ramasubramaniam R and Chen J 2003 *Appl. Phys. Lett.* **83** 2928
[14] Sandler J K W, Kirk J E, Kinloch I A, Shaffer M S P and Windle A H 2003 *Polymer* **44** 5893
[15] Wu G, Lin J, Zheng Q and Zhang M 2006 *Polymer* **47** 2442
[16] Potschke P, Abdel-Goad M, Alig I, Dudkin S and Lellinger D 2004 *Polymer* **45** 8863
[17] Kharchenko S B, Douglas J F, Obrzut J, Grulke E A and Migler K B 2004 *Nat. Mater.* **3** 564
[18] Liu I-C, Huang H-M, Chang C-Y, Tsai H-C, Hsu C-H and Tsiang R C-C 2004 *Macromolecules* **37** 283
[19] Hill D E, Rao A M, Allard L F and Sun Y-P 2002 *Macromolecules* **35** 9466
[20] Krishnamoorti R and Giannelis E P 1997 *Macromolecules* **30** 4097
[21] Agarwal S and Salovey R 1995 *Polym. Eng. Sci.* **35** 1241
[22] Bruck H A and Rabin B H 1999 *J. Mater. Sci.* **34** 2241
[23] Bruck H A and Rabin B H 1999 *J. Am. Ceram. Soc.* **82** 2927
[24] Chong J S, Christiansen E B and Baer A D 1971 *J. Appl. Polym. Sci.* **15** 2007
[25] Krieger I M and Dougherty T J 1959 *Trans. Soc. Rheol.* **3** 137
[26] Rodlert M, Plummer C J G, Leterrier Y and Manson J-A E 2004 *J. Rheol.* **48** 1049
[27] Lin C R and Chen W J 1999 *Colloid Polym. Sci.* **277** 1019
[28] Einstein A 1906 *Ann. Phys., Lpz.* **19** 371
[29] Nielsen L E 1974 *J. Phys. D: Appl. Phys.* **7** 1549
[30] Vassileva E and Friedrick K 2003 *J. Appl. Polym. Sci.* **89** 3774
[31] Lin Y, Meziani M J and Sun Y-P 2007 *J. Mater. Chem.* **17** 1143
[32] Schluter A D 2005 *Functional Molecular Nanostructures: Topics in Current Chemistry* vol 245 (Berlin: Springer)